Time -scale analysis of magnetic field intensity produced by high voltage powerlines

LUIGI MAXMILIAN CALIGIURI
Department of Chemistry and Chemical Technologies
University of Calabria
Via P. Bucci, 87036 Arcavacata di Rende (CS)
ITALY
max.caligiuri@gmail.com

FRANCESCO LAMONACA
Department of Informatics, Electronics and System Engineering
University of Calabria
Via P. Bucci, 87036 Arcavacata di Rende (CS)
ITALY
flamonaca@deis.unical.it

ALFONSO NASTRO
Department of Chemistry and Chemical Technologies
University of Calabria
Via P. Bucci, 87036 Arcavacata di Rende (CS)
ITALY
alfonso.nastro@unical.it

DOMENICA GIORDANO
Department of Chemistry and Chemical Technologies
University of Calabria
Via P. Bucci, 87036 Arcavacata di Rende (CS)
ITALY
domenicagiordano@gmail.com

Abstract: - High voltage powerlines represent one of the most important source of exposition to ELF electrical and magnetic fields for population and environment. The time and frequency analysis of fields produced by such sources is fundamental in order to properly characterize them and correctly evaluate the relative exposition. This is particularly important for fields characterized by different spectral components, for which the exposure limits are specified in function of frequency as stated by the ICNIRP guidelines for limiting exposure to time – varying electric, magnetic, and electromagnetic fields. If the frequency composition of such fields is non – stationary during the measurement time interval, the “traditional” frequency analysis techniques based on simple Fourier transform cannot be applied, but time - frequency and /or time –scale analysis techniques, assuming the signal stationary during a sufficiently small time interval, must be performed. Among these, a great importance have those based on different versions of multiresolution algorithms. The aim of this work is to analyse, by means of such techniques, the time – frequency features of magnetic ELF fields produced by typical high voltage (150 and 220kV) powerlines in their neighbourhood. To such purpose, a set of magnetic broadband field measurements has been performed at specific points placed at difference distances from high voltage wires during a “typical” day (that’s to say during normal operative conditions). Discrete wavelet transform and Daubechies multiresolution algorithms has been applied to the measured fields time history, showing the results obtained respectively using various base atoms system (Gabor, Gauss, Morlet and Franklin atoms in particular) and different Daubechies parameters number. It will be shown how a properly use of these transforms can help us to characterise sources emission especially in order to evaluate human and environmental exposition to ELF magnetic fields.

Key-Words: - Magnetic field, ELF, time – frequency analysis, multiresolution, wavelet, high – voltage powerlines, human exposition.

1 Introduction

High voltage powerlines often represent an important source of exposure to non ionizing radiations for the environmental and population. In a given point, the electrical and magnetic fields intensities, respectively related to the conductors voltage and electrical current load, can show, during a day, considerable variations, caused by the difference between the actual and nominal values. In fact, the actual values of voltage and current load of a conductor can be greater or smaller than the nominal values, depending on wires configuration and energy consumptions. The electrical field time variations are usually caused by transitory voltage drops (of duration between tens of ms and some minutes) with values between 10 and 90% of the nominal value. The magnetic field intensity is directly related to the electrical load of lines, whose values can vary from 30% to 80-90%, with transitory values (of duration of hours) of 200% respect to the nominal value. The fields intensity behaviour furthermore depends on the geometrical disposition of conductors, especially in the presence of different voltage wires. As a result, the electrical and magnetic field intensities show a non stationary trend both in time and frequency. On the other hand, the evaluation of exposition and the expression of the relative field limits has to be made, according to the *ICNIRP* Guidelines [1], as function of field frequency. The spectrum analysis of non –stationary signals cannot be obtained by means of traditional *FFT* - based analysis techniques because they are not able to give us the time localisation of the frequency components of the signal. For this reason we requires the development and application of analysis techniques that get the spectra associated to samples of signal which can be considered sufficiently stationary. Multiresolution analysis represents a technique able to analyse the signal structure at different time - frequency resolutions recognizing its non stationary components [2,3].

In this paper we'll describe the application of wavelet-based multiresolution analysis to the study of the magnetic field intensity time-history [4], measured in the neighbourhood of typical high voltage powerlines (150 and 220kV). It will be shown that a suitable choice of measurement setup and development of multiresolution analysis techniques allow us to properly characterize the time – frequency structure of signal in order to achieve a more realistic evaluation of exposition.

2 Multiresolution analysis applied to signal decomposition

A multiresolution analysis gives a "zoomed" vision of a signal at different scales in such a way that we will dispose of different signal versions each of them characterised by a different detail level. If $L^2(\mathbb{R})$ designs the Hilbert space of square integrable signals $f(t)$, a multiresolution approximation (MRA) for f is a sequence of closed sub-spaces $(V_k)_{k\in\mathbb{Z}}$ such that

$$f(t) \in V_j \Leftrightarrow f(t-2^j k) \in V_j \quad j,k \in \mathbb{Z} \tag{1}$$

$$\forall j \in \mathbb{Z}, V_{j+1} \subset V_j \tag{2}$$

$$\forall j \in \mathbb{Z}, f(t) \in V_j \Leftrightarrow f(2t) \in V_{j-1} \tag{3}$$

$$\bigcap_{j=-\infty}^{\infty} V_j = \{0\} \tag{4}$$

$$\bigcup_{j=-\infty}^{\infty} V_j = L^2(\mathbb{R}) \tag{5}$$

There exists furthermore a function ϑ such that the ensemble $\{\vartheta(t-n)\}_{n\in\mathbb{Z}}$ is a Riesz basis of V_0 that's to say the $\{\vartheta\}_n$ are linearly independent and there exist $A,B>0$ such that, for any $f\in V_0$, one uniquely has

$$f(t) = \sum_{n=-\infty}^{\infty} a[n]\vartheta(t-n) \tag{6}$$

satisfying the property

$$A\|f\|^2 \le \sum_{n=-\infty}^{\infty} |a[n]|^2 \le B\|f\|^2 \tag{7}$$

According to this approach, the approximation of a signal f at scale 2^{-j} can be seen as the orthogonal projection of f on space V_j, and will be denoted by $P_{V_j}f$. Therefore if $\{b_j\}_n$ is an orthogonal basis of V_j we have

$$P_{V_j}f = \sum_{n=-\infty}^{\infty} b_j[n]\phi_{j,n} \tag{8}$$

where $a_j[n] = \langle f, b_{j,n} \rangle$.

It's possible to prove [2] that an orthogonal basis of V_j can be constructed by dilating and translating a function ϕ called "scaling" function; if $(V_k)_{k\in\mathbb{Z}}$ is an MRA and ϕ is the scaling function whose Fourier transform is

$$\hat{\phi}(\omega) = \frac{\hat{\vartheta}(\omega)}{\left(\sum_{k=-\infty}^{\infty}\left|\hat{\vartheta}(\omega + 2k\pi)\right|^2\right)^{1/2}} \tag{9}$$

then the functions $\{\phi_{j,n}\}_{n\in\mathbb{Z}}$ where

$$\phi_{j,n}(t) = \frac{1}{\sqrt{2^j}}\phi\left(\frac{t-n}{2^j}\right) \tag{10}$$

represent an orthogonal basis of V_j. A *MRA* is then completely defined by means of the scaling function ϕ that generates an orthogonal basis for each space V_j. If we indicate with W_j the orthogonal complement of V_j in V_{j-1} we can write

$$V_{j-1} = V_j \oplus W_j \tag{11}$$

and the approximation of f at scale 2^{j-1} $P_{V_{j-1}}f$ is given by

$$P_{V_{j-1}}f = P_{V_j}f + P_{W_j}f \tag{12}$$

The projection $P_{W_j}f$ gives us the informations about the "details" of the signal at scale 2^{j-1} that we cannot "view" at less accurate scale 2^j. It has been shown [2] that an orthonormal basis of W_j can be constructed by means of the so called "wavelets" waveforms. The projection of a signal f in the "detail" space W_j is given by an expansion in terms of wavelet basis $\{\psi_j\}_n$

$$P_{W_j}f = \sum_{n=-\infty}^{\infty}\langle f, \psi_{j,n}\rangle \psi_{j,n} \tag{13}$$

A signal f can be then expressed as composition of the "details" at all scales

$$f = \sum_{j=-\infty}^{\infty} P_{W_j} = \sum_{j=-\infty}^{\infty}\sum_{n=-\infty}^{\infty}\langle f, \psi_{j,n}\rangle \psi_{j,n} \tag{14}$$

we know an orthogonal wavelet basis

2.1 Wavelet basis

A continuous *wavelet* is a function $\psi \in L^2(\mathbb{R})$ such that

$$\int_{-\infty}^{\infty}\psi(t)dt = 0 \tag{15}$$

$$\int_{-\infty}^{\infty}\frac{\left|\hat{\psi}(\omega)\right|^2}{|\omega|}d\omega < \infty \tag{16}$$

(where $\hat{\psi}$ is the Fourier transform of ψ) usually normalised $\|\psi\| = 1$ and centred in the neighbourhood of $t = 0$. A wavelet "family", whose elements are called "atoms", is obtained by translating ψ by u and by "scaling" ψ by a factor s:

$$\psi_{u,s}(t) = \frac{1}{\sqrt{s}}\psi\left(\frac{t-u}{s}\right) \tag{17}$$

with $\|\psi_{u,s}\| = 1$. The continuous wavelet transform of a signal $f(t)$ is the image $WT^{\psi}[f](u,s)$ on $]0,\infty[\times\mathbb{R}$ given by

$$\begin{aligned} WT^{\psi}[f](u,s) &= \langle f, \psi_{u,s}\rangle = \\ &= \int_{-\infty}^{\infty} f(t)\psi^*\left(\frac{t-u}{s}\right)dt \end{aligned} \tag{18}$$

(where * indicates the conjugate complex) and quantifies the contribution of the signal f in the neighbourhood of $t = u$ at a scale s. The time translation of atoms permit to us to select the different portions of signal while by dilating and contracting it we are be able to analyse signal structures of very different size. When the atoms are dilated we analyse the signal components oscillating more slowly while when they are contracted we can analyze the components oscillating more quickly.
We can construct a wavelet function such that the family of translated and scaled functions

$$\left\{\psi_{j,n}(t) = \frac{1}{\sqrt{2^j}}\psi\left(\frac{t-2^j n}{2^j}\right)\right\}_{j,n\in\mathbb{Z}} \tag{19}$$

is an orthonormal basis of $L^2(\mathbb{R})$. The basis can be obtained from a scaling function ϕ

$$\hat{\psi}(\omega) = \frac{1}{\sqrt{2}}\hat{\phi}\left(\frac{\omega}{2}\right)\hat{g}\left(\frac{\omega}{2}\right) \tag{20}$$

with

$$\hat{g}(\omega) = e^{-i\omega}\hat{h}^*(\omega + \pi) \tag{21}$$

where h represents the conjugate mirror filter[1] corresponding to ϕ.

[1] A conjugate mirror filter can be defined as a discrete filter whose transfer function satisfies the condition $\forall\omega \in \mathbb{R}, \left|\hat{h}(\omega)\right|^2 + \left|\hat{h}(\omega+\pi)\right|^2 = 2$.

The multiresolution approach and its realization by means of wavelet basis leads [3], first of all, to a time – scale decomposition. Nevertheless we can "convert" it into a time – frequency signal decomposition, by properly choosing the wavelet basis. We can establish such a relationship between scale and frequency by assuming that the base function is placed, in the frequency domain, around a frequency ω_0, corresponding to the maximum value of the wavelet frequency spectrum. The simultaneous time-frequency resolution of analysis is limited by the Heisenberg uncertainty principle:

$$\Delta\omega\Delta t \geq \frac{1}{2} \tag{22}$$

where the time resolution Δt is related to the wavelet time spread Δt_ψ (with $\Delta t = s\Delta t_\psi$) and the frequency resolution to the wavelet bandwidth $\Delta\omega_\psi$ ($\Delta\omega = \Delta\omega_\psi / s$). The product $\Delta\omega\Delta t$ and so the effectiveness of the analysis depends on the wavelet waveform shape and parameterization. To analyse the signals associated to electric and magnetic fields, some classes of wavelet atoms, with Fourier transforms obtained from equation (20), have been employed.

They are the Gauss, Morlet, Gabor, Franklin and Daubechies wavelets. The *Gauss* wavelet is the function whose Fourier transform is given by

$$\hat{\psi}_{Gauss}(\omega) = \exp\left[-\omega^2 / 2\right] \tag{23}$$

the *Gabor* wavelet is a "phase displaced" version of a gaussian function

$$\hat{\psi}_{Gabor}(\omega) = \exp\left[-\left(\omega - \omega_0\right)^2 / 2\right] \tag{24}$$

with $\omega_0 = \pi\sqrt{2/\log 2}$. In the same way we can define the *Morlet* and *Franklin* atoms

$$\begin{aligned}\hat{\psi}_{Morlet}(\omega) &= \exp\left[-\left(\omega - \omega_0\right)^2 / 2\right] + \\ &-\exp\left[-\left(\omega + \omega_0\right)^2 / 2\right]\end{aligned} \tag{25}$$

$$\begin{aligned}\hat{\psi}_{Frank}(\omega) &= \cos\left(\frac{\pi\omega}{16}\right)\sin\left(\frac{\pi\omega}{16}\right)^2 \times \\ &\times\sqrt{\frac{2-\cos\left(\pi\omega/16\right)}{\left[2+\cos\left(\pi\omega/16\right)\right]\left[2+\cos\left(\pi\omega/8\right)\right]}} \times \\ &\times\left[\sin c\left(\frac{\pi\omega}{8}\right)\right]^2\end{aligned} \tag{26}$$

The *Daubechies* multiresolution analysis is based on the so-called "Daubechies pseudo-filters" of order $2p > 0$ built by means of trigonometric polynomials

$$\hat{h}(\omega) = \sqrt{2}\left(\frac{1+e^{-i\omega}}{2}\right)^p \prod_{k=0}^{m}\left(1 - \alpha_k e^{-i\omega}\right) \tag{27}$$

3 Magnetic field sources and experimental data

We know that the highest signal frequency component $f_{\max}$ we can analyze is proportional to the sampling frequency. For a windowed discrete FFT transform, for example, we have

$$f_{\max} = \pi f_{samp} \tag{28}$$

where f_{samp} is the sampling frequency.

In order to analyze the highly non-stationary phenomena, such as the fast transients, we have to sample the signal at a sufficiently high frequency; for example, using the above relation for $f_{\max} = 100kHz$ we obtain a sampling frequency of order of $3 \times 10^5 Hz$.

Almost all the commercial low-frequency fields analyzers don't offer this possibility giving us the RMS values of fields intensity [4,5,6]. For this reason we have realized, in order to collect the required data, an experimental apparatus provided for the purpose able to measure, for each axis, the "instantaneous" field intensity at the required sampling frequency. It is made up of a detector (a coil and a conductive disk respectively for the magnetic and electrical field, opportunely shielded) coupled to an amplifier stage connected to a PC by means of an acquisition A/D converter board [4]. The sampled data have been numerically treated through a set of routines performing the signal multiresolution decomposition. We'll describe in this paper, for briefness sake, only the results obtained for magnetic fields, since the procedures and conclusions relative to electric field measurements are quite similar.
The site under investigation is schematically shown in Fig. 1, in which AT_1 represents an high voltage wire (nominal voltage $V = 150kV$), characterized by an opposite double threesome conductors configuration, AT_2 and AT_3 two high voltage wires (same nominal voltage) characterized by a single threesome conductors configuration, MT_1, MT_2 and MT_3 three low voltage wires (nominal voltage $V = 20kV$) characterized by a single threesome conductors configuration

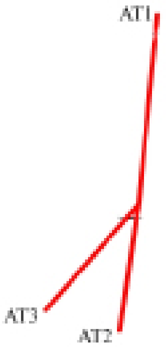

Fig. 1. Schematic configuration of conductor lines

The measurements have been carried out at a set of points situated in the neighbourhood of the central, at different distances to the main high and low voltage wires, during a "typical" day (that's to say under operative conditions practically coinciding with the mean ones) and under the following mean climatic conditions: $t = 30^{\circ}C$ and relative humidity of 65%. In this paper we'll describe the results obtained at the P_1, placed on AT_1 axis at $h = 1.5m$ above the ground and distance $d = 10m$ in front of the station perimeter.

The Fig.2 shows the overall magnetic field time – history s_1 measured at P_1, using a sampling frequency $f = 44100Hz$ during a time interval $\Delta T_1 = 10s$; on the x-axis is represented the sample number N, on the y-axis the normalized signal amplitude, in arbitrary units.

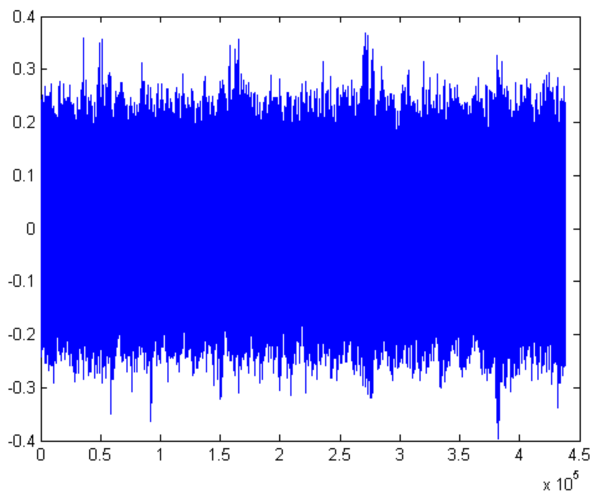

Fig. 2. Time history of magnetic field intensity s_1

In the Fig. 3-6 are shown the time-scale representations corresponding to the continuous Wavelet transform of the signal s_1 obtained for different choices of wavelet base atoms. On the x axis is represented the time interval normalized between 0 and 1, on the y axis the quantity $h = \log_2(1/s)$ usefully related to the scale factor s and the image points intensity is proportional to WT coefficients (the intensity growing from black to yellow).

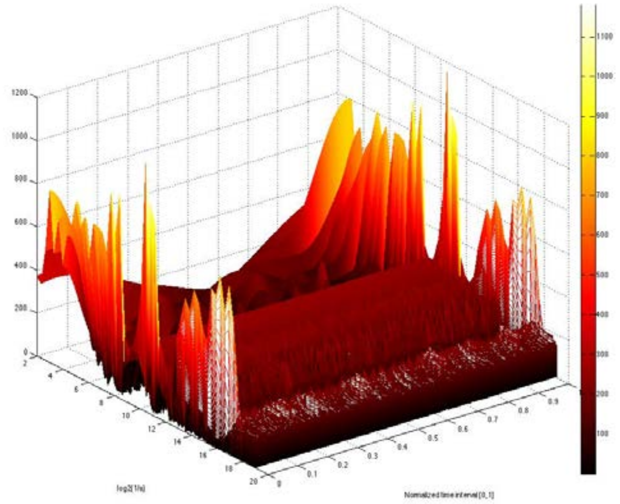

Fig. 3. WT of signal s_1 using Morlet base atoms

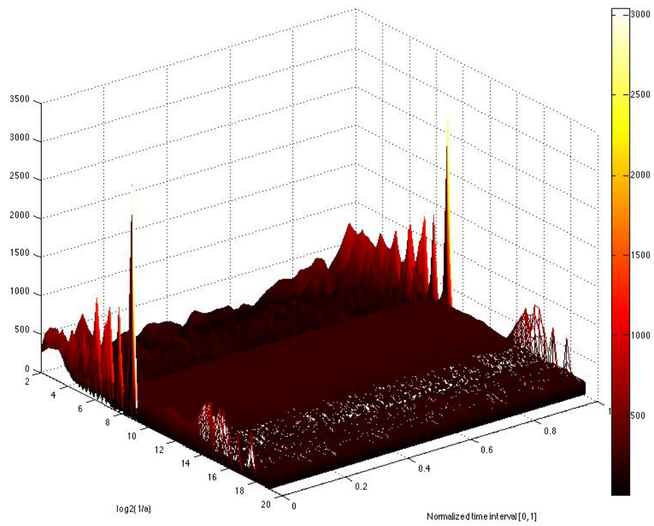

Fig. 4. WT of signal s_1 using Franklin base atoms

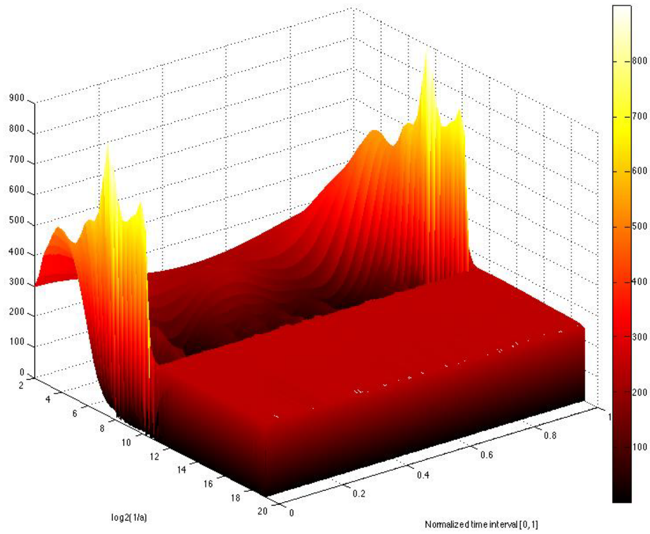

Fig. 5. WT of signal s_1 using Gauss base atoms

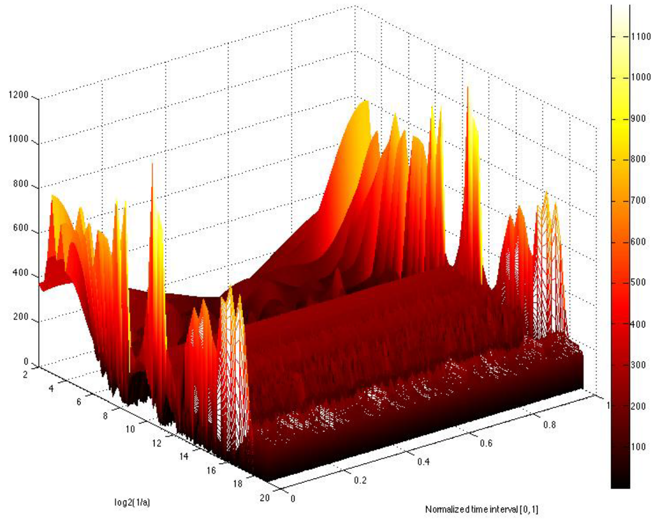

Fig. 6. WT of signal s_1 using Gabor base atoms

We note, first of all, that a lot of details in time-scale images strongly depend on the particular wavelet chosen, and that, in this case, the Morlet wavelet (immediately followed by Gabor wavelet) achieves the best compromise between time and scale resolution, highlighted by the image clearness in the time and scale ranges. In this type of analysis the high-scale components (corresponding to the low frequencies) are always characterized by poor time resolution (and correspondingly high frequency resolution) while low-scale components (corresponding to the high-frequencies) have a poor frequency resolution (and correspondingly high time resolution). In particular, the Fig. 3 puts in evidence the presence, at high and middle scale values (h between about 8 and 10), of a structure remaining basically stationary during the whole time interval ΔT_1, that is due to a set of closely spaced frequency components of comparable intensity including the fundamental frequency component (50Hz) of the signal. The analysis also shows the presence of non-stationary components at finer scales (h between about 10 and 13) and fast transients at the highest scales (h greater than about 18) for the whole time interval, associated to the current spikes of powerline. For values of h lower than about 6. we see the presence of many non – stationary components whose amplitude considerably varies during measurements, these components area associated to electric current instabilities in the powerline and to measurement device electrical noise. These features are substantially confirmed by the results of Fig. 4 and Fig. 6. Finally we can recognize an “atypical” field event, characterized by a particular time-scale configuration around $t = 0.6$. Finally we note, in this case, the Gauss base atoms are not suitable for the analysis since, from Fig. 5 we can see it is not be able to resolve the time – scale patterns in the low and medium scale ranges (for $h > 8$) and the presence of peaks, in time, in the high scale range.

In the Fig. 7-8 is shown the “details” decomposition (13) of s_1, obtained by means of a 8-parameters Daubechies multiresolution analysis, at different detail levels d_1, d_2, d_3, d_4, d_5. On the x axis is represented the sample number N, on the y axis the signal amplitude in arbitrary units. We see that the low-scale detail d_1 practically corresponds to the signal itself and so gives us no further informations about it.

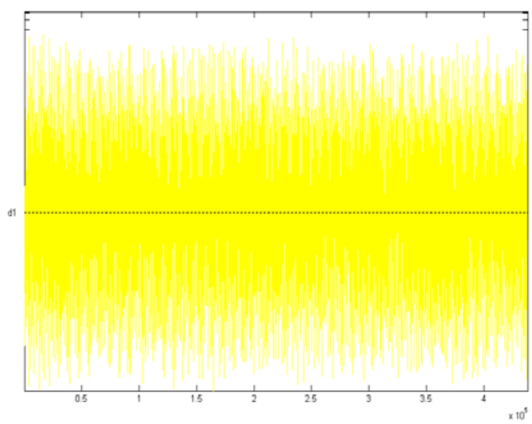

Fig. 7. 4-parameter Daubechies multiresolution analysis of s_1 (d1 detail)

The analysis shows a low scale stationary pattern (h between about 9 and 10.5), that now appears broader in the scale domain, suggesting the presence of more spaced set of frequency components including the fundamental one. Further nearly-stationary components are placed around $h = 11.5$ while non stationary and transients structures are again present at lower scale values. Particularly evident is also the "atypical" field structure occurred around $t \simeq 0.25$, whose presence is confirmed by the analysis of the d_3 and d_4 details (see Fig. 7) around the sample value $N = 1.15 \cdot 10^5$.

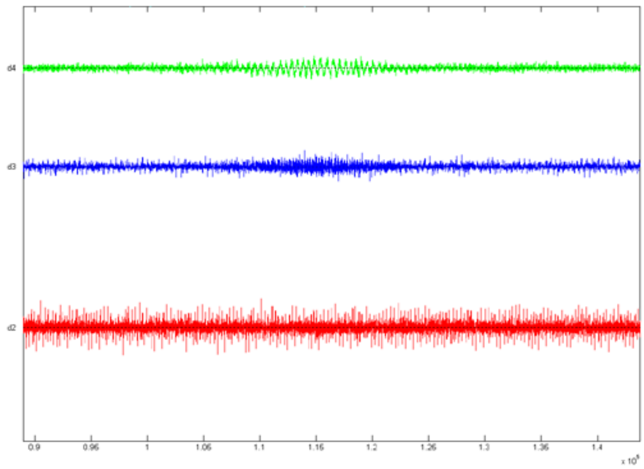

Fig. 8. 8-parameter Daubechies multiresolution analysis of s_1 (d2-d5 details)

4 Conclusions

Multiresolution analysis permits an accurate decomposition of the signal into a set of "details" waveforms components that can isolate all scales (or frequencies) of signal structures from the largest to the smallest pattern of variation in time of the signal. Time-scale representations permit us to search for significant patterns or events at specific scales (or frequencies) and to view time relationship between them. As we have seen, by selecting appropriate wavelet atoms and Daubechies parameters, we can properly analyze the time-frequency structure of electric and magnetic fields generated in the neighbourhood of a transformation station. The analysis has shown the presence of coherent structures (consisting of low-frequency stationary components and non-periodic patterns) as well as highly non –stationary components and singularities. These informations about the fields behaviour can have a great importance in evaluating the exposition to such fields, since it strongly depends on the frequency fields composition. In fact the "traditional" techniques, all mainly based on the signal RMS integration, are not able to reveal these frequency components. On the other hand, they could have even more importance in the case of higher voltages powerlines as the 380 and 220 kV ones, especially in the surrounding of power and transformation stations or when two or more lines of equal or difference voltages and current phase intersect each other. In these cases, the sensibility of the proposed methods to the "spurious" (i.e. different from the main harmonic at 50 / 60 Hz) strongly depends on the choice of the correct Daubechies parameter and detail. In this sense one of strengths of the proposed approach is that it doesn't need for a preliminary signal denoise since it is automatically performed by multiresolution analysis itself as we have seen in the shown results. This is particularly evident in the 8 – parameters analysis (d_4 detail) able to "isolate" the atypical events in the signal time history.

In applying multiresolution techniques we must remember that they leads to a frequency analysis with constant percentage bandwidth whose value depends on the wavelet atom shape and parameterisation used for the analysis. The choice has to be made in function of the signal features, so, in performing it, it's necessary to have a sufficient preliminary knowledge of signal to be analyzed.

For example, in this case, we have seen the use of Gauss base atoms is completely unsuitable in order to extract the main signal features and then, in comparison with the other types of bases considered. This also suggests the opportunity, when facing with signals whose time – frequency features are not known a priori,

Furthermore, in the case of long signals, their numerical implementation can present great computational problems. Fortunately, these knowledge can be more easily obtained by preliminary performing a "traditional" time-frequency analysis, as for example a WDFT (Windowed Fourier Discrete Transform) whose numerical realisation is more simple. To overcome this limitations we are studying modified versions of the multiresolution algorithms able to guarantee a faster implementation and so a wider applicability, also to others electric and magnetic field sources.

References:

[1] ICNIRP: *"Guidelines for limiting the exposure to time-varying electric, magnetic and*

electromagnetic fields (up to 300 GHz)", Health Physics, Vol. 74, No. 4 (1998).

[2] S. Mallat, *A wavelet tour of signal processing*, Academic Press (1999).

[3] Y. Meyer, *Wavelet Algorithms and Applications*, SIAM, Philadelphia (1993).

[4] Luigi M. Caligiuri, A. Sabato, *Multiresolution analysis of electric and magnetic fields generated by a typical electrical transformation station for energy distribution*, Proceedings of IRPA 11, The 11th Congress of the International Radiation Protection Association, 23 – 28 May, Madrid, SPAIN.

[5] IEEE Std. 644-1994: "*IEEE Standard Procedures for Measurements of Power Frequency Electric and Magnetic Fields from AC Power Lines.*

[6] IEEE Magnetic Fields Task Force Report: "*A Protocol for Spot Measurements of Residential Power Frequency Magnetic Fields"*, IEEE Transaction on Power Delivery 8, pp. 386-1394 (1993).